Strain and confined resonances in ultrathin alkali-metal films

E. Hulpke and J. Lower*
Max-Planck-Institut für Strömungsforschung, D-37073 Göttingen, Germany

A. Reichmuth
Cavendish Laboratory, Madingley Road, Cambridge CB3 OHE, United Kingdom
(Received 12 October 1995)

We have investigated the structure and lattice dynamics of ultra-thin alkali-metal films in the systems K/Ni(001) and Cs/Cu(111) using the technique of high-resolution helium atom scattering (HAS). Our results are compared with those from an earlier HAS study of Na/Cu(001). For all of these systems, lattice mismatch at the substrate/film interface introduces strain in the films which is found to be gradually removed during the growth process. Our comparative study shows that relaxation of the alkali-metal films into the bulk alkali metal occurs more rapidly as one proceeds from Na to K and Cs. The presence of strain relief is revealed in our observations of a layer-dependent Debye-Waller effect, the Debye temperature in the film decreasing with increasing film thickness from values close to that of the substrate to the bulk alkali-metal Debye temperature. More detailed information on strain relief in the alkali-metal films is provided by the variations in their vibrational frequencies with increasing film thickness. As for the Na/Cu(001) system, the K and Cs films investigated here exhibit prominent confined vibrational resonances. Our results show that measurements of the vibrations of atoms in the film surface yield information not only on the force constants at the film surface but also on those within the film itself. Comparison of results between the different alkali-metal systems elucidates further the nature of the growth process, the development of strain relief during growth, and the behavior of confined vibrational resonances.

I. INTRODUCTION

Alkali-metal adsorption on metals at coverages in the submonolayer regime has been extensively studied in the past and is reviewed in a recent article by Diehl and McGrath.[1] The great interest in these systems is due to questions concerning the charge transfer on adsorption[2,3] and to the role alkali-metal atoms play in heterogeneous catalysis.[4] Considerably less work in the literature is related to alkali-metal films with thicknesses exceeding one monolayer (ML). The pioneering study of Andersson *et al.*[5] has shown that on further deposition epitaxial Na films can be grown on a Ni(001) substrate. Such an *in situ* growth of alkali-metal single crystals provides a unique opportunity to prepare well ordered and clean surfaces of these fundamentally interesting metals.[6,7]

More recently, helium atom scattering (HAS) was applied to investigate the growth of Na films deposited on Cu(001) (Ref. 8) and of Na, Rb, and Cs films on a graphite surface.[9,10] The work of Benedek *et al.*[8] revealed the existence of interesting vibrational modes in the alkali-metal films which were, according to the surface sensitivity of HAS, attributed to collective motions of atoms in the film surface. These modes exhibit the behavior of Einstein oscillators as their frequencies do not depend on the amount of parallel momentum transferred to the surface in the course of the helium scattering. The authors[8] explain this phenomenon in terms of the formation of standing longitudinal acoustic waves perpendicular to the film resulting in the observed shear vertically polarized ''in phase'' oscillations of surface atoms. The frequencies of these open standing-wave modes and their overtones depend distinctly on the film thickness and contain information on interatomic force constants in the film and at the interface to the substrate.[11]

The work presented here is an extension of these HAS studies to other alkali-metal–substrate systems. It will be shown that a comparison between systems with different bulk and interface force constants leads to an even better understanding of the confined vibrational modes. Comparing the vibrational properties also provides insights into the amount of strain in the films caused by the misfit of lattice parameters at the interface and into how this strain is removed in the course of film growth.

In Sec. II the techniques employed to prepare the crystal substrate and deposit the alkali-metal layers are described. Section III describes how the HAS technique is used to both monitor crystal growth during deposition and characterize the film surface in terms of its structure and degree of order. In the course of monitoring the film growth using HAS, very interesting changes in the Debye-Waller attenuation of scattering intensities on changing the film thickness were found which are indicative of film strain and its relaxation on continuing growth. In Sec. IV, results from the study of the vibrational spectra of ultrathin alkali-metal films as a function of their thickness are presented. As previously observed in the Na/Cu(001) system, film modes of Einstein oscillator character were also found in K and Cs films. Section V contains a comparison of the film mode data for the three systems and their discussion in terms of film strain and its relief. Also discussed are the implications of these data for an adequate description of the confined vibrational resonances in the films.

II. EXPERIMENTAL DETAILS

The HAS apparatus used for the experiments on K/Ni(001) and Cs/Cu(111) is similar to the one used for Na/Cu(001) and is described elsewhere.[12] A separate UHV chamber was used for the LEED studies on Na/Cu(001),[13] whereas for K/Ni(001) and Cs/Cu(111), LEED and HAS were integrated in one system.

The single crystal substrates (purchased from Kelpin, D-69181 Leimen) were cleaned by cycles of 800 eV Ar^+ sputtering and annealing to 800 K for copper and 1100 K for nickel. The main contaminant on copper was sulfur, which could be removed by heating the crystal in a hydrogen atmosphere of about 10^{-6} mbar. After the cleaning process no contamination related peaks could be resolved with Auger electron spectroscopy. The total helium specular reflectivity was about 0.15 and the angular half-width of the specular peak did not exceed the resolution of the apparatus of 0.2°. Hence, a terrace size of at least several 100 Å can be assumed for all substrates.

The alkali metals were evaporated from getter dispensers (SAES) mounted about 60 mm away from the substrates. A shutter could be placed between dispensers and substrates in order to block the impinging alkali-metal beam. The dispensers were carefully degassed and warmed up slightly below their operating temperature more than 1 h before each experiment. The operating temperature was stabilized by setting it about 5 min before the shutter was opened for deposition. Before each recleaning cycle by sputtering and annealing, the crystal was exposed to oxygen as it was found that in this way an optimum specular helium reflectivity could be achieved. Although the reason for this improvement is not clear, it is suspected that the oxygen atoms serve to hinder the migration of alkali-metal atoms from places on the crystal or the crystal holder, not in sight of the sputter gun, back onto the cleaned crystal surface during the annealing phase.

III. EPITAXIAL GROWTH

A. Growth mode

The specular helium reflectivity during alkali-metal adsorption—referred to simply as reflectivity below—was monitored for all systems and typical results are shown in Fig. 1. Oscillations are visible in the reflectivity versus exposure time curves at sufficiently low temperatures [150 K for Na/Cu(001), 100 K for K/Ni(001), and 75 K for Cs/Cu(111)]. We interpret the appearance of these oscillations as an indication for a layerwise growth in agreement with previous growth studies using helium atom scattering on other systems.[14–16] The maxima in the reflectivity correspond to films consisting of an integral number of layers. Here we define 1 ML as the most densely packed layer for which all alkali-metal atoms are in direct contact with the substrate. Coverages in between lead to a film surface containing a larger density of defects which scatter helium atoms diffusely away from the specular direction.

A slight variation in the separation of the maxima as well as an attenuation in reflectivity with increasing coverage indicate that the growth is not entirely perfect: A new layer starts to grow before the previous layer has been fully completed. Still, the appearance of distinct oscillations makes repeatable coverage determinations possible, with an accuracy of at least 0.1 ML. An additional factor contributing to the intensity loss with increasing coverage is the change in the Debye temperature of the film which will be discussed in the following section.

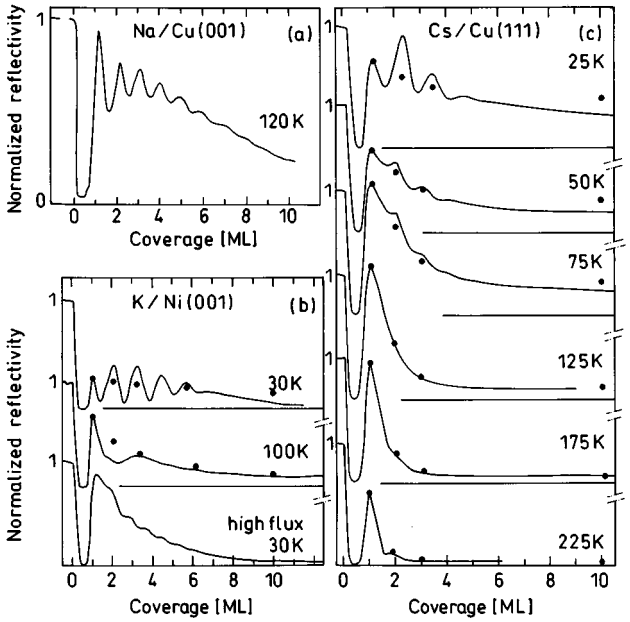

FIG. 1. Deposition curves: normalized specular He atom reflectivity versus coverage for different systems and experimental conditions. (a) Na/Cu(001). Deposition rate 0.015 ML/sec, He beam energy E_i=12.5 meV (in-phase condition) substrate temperature 120 K. (b) K/Ni(001). Deposition rates for top traces, 0.02 ML/sec; bottom trace, 0.1 ML/sec. He beam energies from top to bottom: 17.5 meV (in-phase), 28.7 meV (out-of-phase), 17.5 meV (in-phase), substrate temperatures as indicated. The symbols show that the attenuation in reflectivity with increasing coverage is due solely to the thickness dependent Debye-Waller effect (cf. Fig. 2 and the text). (c) Cs/Cu(111). Deposition rates 0.02 ML/sec, He beam energy 28.5 meV (in-phase), substrate temperatures and symbols as before.

The occurrence of Frank-van-der-Merwe growth is thermodynamically expected in these systems when the surface free energies of the metals are considered [0.81 eV for Ni(001), 0.64 eV for Cu(001), 0.18 eV for Na(110), 0.16 eV for K(110), and 0.14 eV for Cs(110) (Ref. 17)]. The surface energy of the substrate significantly exceeds that of the adsorbate in all systems studied and it would take an unrealistically large interface energy to violate Bauer's criterion for layerwise growth.[18] Thus, the reason for nonperfect layer by layer growth is either that the migration of adsorbed atoms at the given temperature is too slow or that the lattice mismatch between substrate and adlayers is too large, resulting in strained adlayers.

B. Temperature effects

The helium reflectivity during alkali-metal deposition is found to be strongly temperature dependent, as can be seen in Fig. 1. The oscillations become less pronounced as the sample temperature is raised and the average reflectivity decreases. The weaker oscillations alone could reflect the fact

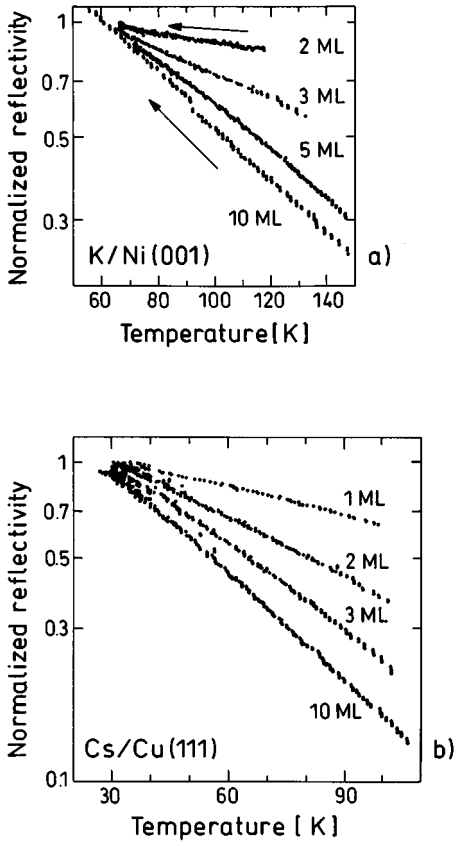

FIG. 2. Temperature dependence of the normalized specular He reflectivity for films of various numbers of completed monolayers. Top panel, K/Ni(001); bottom panel, Cs/Cu(111). The curves were obtained after deposition of N completed monolayers at 30 K, followed by annealing to 180 K and on cooling the films. The slope in these semilogarithmic plots contains the surface Debye temperature, which obviously depends on the film thickness.

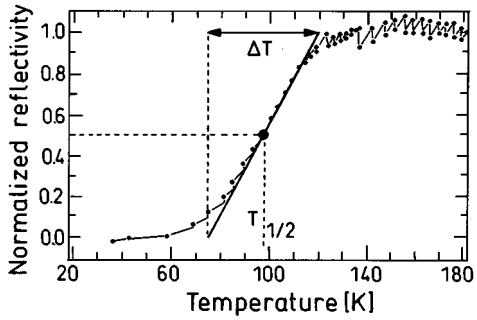

FIG. 3. Changes in the specular He reflectivity on annealing a 10 ML K film deposited on Ni(001) at 30 K. The attenuation due to the Debye-Waller effect for 10 ML has been eliminated from the raw data. The surface temperature is varied linearly with time at a rate of 0.8 K/sec. Barrier heights for interlayer diffusion can be extracted from the position of the point of inflection, $T_{1/2}$, and the slope of the curve at this point (cf. Ref. 21).

that the growth gradually changes character with rising temperature, from a situation where two-dimensional (2D) islands are formed to step flow where the step density, and hence the reflectivity, stays constant with coverage.

In order to elucidate the reasons behind this trend towards lower reflectivity at higher temperatures, films of various thicknesses were prepared on cold substrates, annealed at higher temperatures to reduce the concentration of defects, and their reflectivity was then measured as a function of slowly decreasing temperature. Figure 2 shows the change in reflectivity during cooling for K/Ni(001) and Cs/Cu(111). Given that the temperature dependence is almost exponential, as would be expected from the Debye-Waller effect, the Debye temperature Θ_D was extracted according to the familiar expression for the Debye-Waller exponent

$$2W = \frac{3\mathbf{k}^2 k_B T}{M\omega_D^2} \tag{1}$$

with $\mathbf{k}$, the amount of perpendicular momentum transfer, T the surface temperature, k_B Boltzmann's constant; M the mass of the alkali-metal atom, and $\omega_D = k_B\Theta_D$ (cf. Ref. 19). The values [K/Ni(001): 250/155/160/107 K and Cs/Cu(111): 81/68/53/48 K, for 2/3/5/10 ML] indicate a continuous decrease of the Debye temperature with adsorbate coverage, from the value for the bare substrate to values close to those of the bulk of the adsorbate at about 10 ML. The results of these measurements are also plotted in Fig. 1, where symbols show the Debye-Waller factors scaled so that at 1 ML coverage the values for the Debye-Waller factors and the reflectivity curves coincide. These results show the attenuation in reflectivity expected from the layer-dependent Debye-Waller effect alone.

Considering the Debye temperatures of the substrates used in this work [375 K for Ni and 315 K for Cu (Ref. 20)] and those of the thick alkali-metal films shown above, the ranges in which the Debye temperatures vary during film growth become considerably larger as one proceeds towards the heavier alkali-metal adsorbates. Thus the decrease in reflectivity during film growth becomes more pronounced as the atomic number of the adsorbate increases, which may also explain why the number of evident oscillations is larger in the case of Na (about 8) than in K (about 6) and cesium (only 4).

However, for thick films (10 ML) and at the lowest temperatures (30 K and 25 K, respectively) the Debye-Waller effect is not sufficient to explain the low reflectivities in Fig. 1. We have measured the helium reflectivity in the course of the annealing process by slowly raising the temperature of a film deposited on a cold substrate. Figure 3 shows the reflectivity behavior, which has been corrected for the Debye-Waller effect, during that process for a 10 ML layer film of potassium on Ni(001). The corrected intensity does not stay constant but increases in a ''steplike'' fashion. The most likely explanation for this behavior is that defects are removed due to the increased migration of adatoms.

The position of the point of inflection in this curve, $T_{1/2}$, and the slope at this point can be used to roughly estimate the energy barrier for diffusion as discussed in Ref. 21. The values (38 ± 12 meV for potassium and 24 ± 12 meV for cesium) appear to be plausible when compared with a recent determination of the energy barrier for sodium diffusion on Cu(001) (51 meV).[22] We do not expect the diffusion barrier for an alkali-metal atom on a bare substrate to be smaller than on the alkali-metal film itself given the stronger bond between alkali-metal atom and substrate.

Finally, the shape of the reflectivity curves in Fig. 1 for

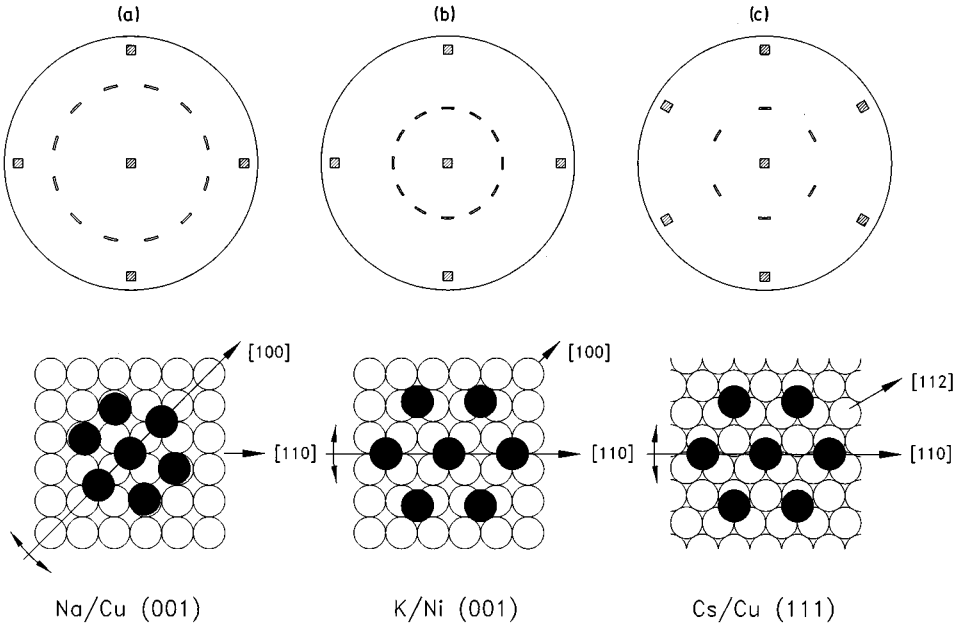

FIG. 4. Top row: schematic LEED patterns obtained from ultrathin films of thicknesses between 2 and 10 ML. The ''spots'' marked by square symbols indicate the diffraction patterns of the substrates which are not seen in LEED for films thicker than 2 ML. Bottom row: structure models for the film surface. (a) Na/Cu(001); (b) K/Ni(001); (c) Cs/Cu(111). Open circles, arrangement of the substrate atoms; filled circles, position of atoms in the top layer of the film in quasihexagonal structures; double arrows, possible misalignment of film domains with respect to high symmetry directions in the substrate causing the broadening of the LEED spots; for details see the text.

Cs/Cu(111) at 175 and 225 K yields further support for the points made above. Following the first oscillation, the reflectivity curves appear to decrease linearly with coverage with a different slope for each new monolayer. The temperatures are well above the temperature for the annealing process. It can safely be said that the growth is not hindered due to limited migration of adatoms. We consequently assume that growth takes place in a step flow mechanism. Although the morphology of the surface is not changing (as it does for 2D island growth at lower temperatures), the fraction of the substrate covered with an additional layer increases continuously. Since the Debye-Waller attenuation depends on the film thickness, the observed reflectivity is a weighted sum of the reflectivities for a film with N layers and a film with $N+1$ layers, with the weight factor being proportional to the respective area covered. This of course leads to a straight line between the reflectivities for the pure N layer and the pure $N+1$ layer film.

C. Lateral structure

None of the prepared alkali-metal films for coverages >1 ML showed helium diffraction peaks related to an atomic corrugation. Thus, the surface corrugation of the electron density must be far less than 10^{-4} Å given the dynamic intensity range of at least 10^{-5} of the apparatus. LEED had to be used in order to gain information on the lateral film structure.

For Na/Cu(001) at 1 ML a $c(2\times2)$ LEED pattern was obtained.[13] For 2 and more monolayers a ring of 12 adsorbate related spots was observed as shown in Fig. 4(a). The ring was oriented in such a way that spots could be found in the $\langle 100\rangle$ directions of the Cu(001) substrate. The intensities of all 12 spots were equal and were all slightly broadened in the azimuthal direction, even after long annealing.[13] We interpret the diffraction pattern, in agreement with the previous results for Na/Ni(001),[5] as a superposition of those from two hexagonal rotational domains. The orientation of the hexagons is determined by the small mismatch between the bulk sodium nearest neighbor distance and the copper atom distance along the $\langle 100\rangle$ direction. The azimuthal broadening of the spots could be caused by small rotations of the hexagons away from the $\langle 100\rangle$ axis indicated by the arrows in Fig. 4(a). Such a rotation with respect to the substrate has been observed before for adsorbed alkali metals.[23]

The results for K/Ni(001), presented in Fig. 4(b), are observed to be somewhat similar to those for the Na/Cu(001) system, the ring of 12 adsorbate related spots again being interpreted in terms of hexagonal adsorbate domains. In contrast to the results for the K/Ni(001) system, however, the 12 spots here were observed for all levels of adsorbate coverage and the magnitude of azimuthal broadening, which was measured to be around 10° for a coverage of 1 ML, was found to decrease with increasing adsorbate coverage, indicating a reduction of the the angle of rotation during growth. In addition, the alignment of the adsorbate spots with respect to the substrate was found to be different in the two systems, in the case of K/Ni(001) the spots being oriented along the $\langle 110\rangle$ directions of the substrate. The reason for this orientation is the small difference between the nearest neighbor distance in bulk potassium and twice the nickel atom spacing along the $\langle 110\rangle$ direction. Again it seems reasonable to assume that the angular broadening is due to rotations in the hexagonal potassium superstructure away from the Ni$\langle 110\rangle$ axis by angles ranging between $\pm 5°$. We note that a rotation of about about 5° was found for a 1 ML coverage in a previous LEED study for this system[24] while the results of recent LEED studies[25] show that above 2 ML a pattern of broad spots, located on two concentric rings, is observed, indicating a distortion of the hexagons towards an arrangement of atoms in a bcc (110) surface.

Cs/Cu(111) showed a $p(2\times2)$ superstructure [see Fig. 4(c)]. The six observable spots were again broadened in the azimuthal direction although low spot intensities made observations difficult. [The appearance of only 6 instead of 12 spots reflects the hexagonal symmetry of Cu(111).]

In summary, the alkali metals form hexagonal domains above 1 ML for all systems studied here. The broad LEED

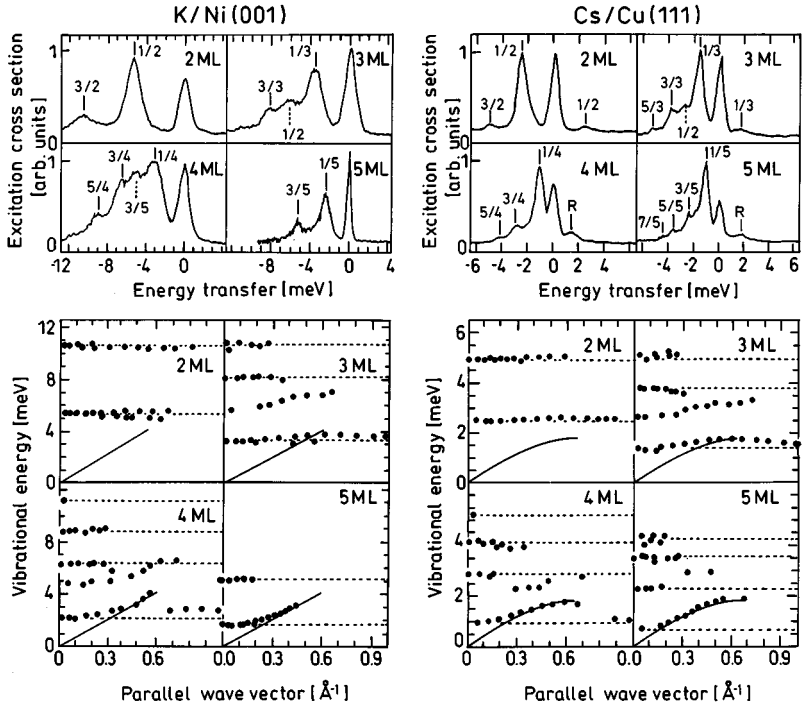

FIG. 5. Film modes: collective vibrations on the surfaces of thin alkali-metal films. Top row: energy transfer spectra for inelastic He scattering close to specular reflection for various film thicknesses, labeling of the peaks according to the open standing wave notation (see the text). Right hand column, Cs/Cu(111) data; left hand column, K/Ni(001) data. Bottom panels: dispersion of the film modes, vibrational energies versus the parallel momentum transferred to the surface. The solid lines indicate the lowest bulk phonon band edge of the respective alkali-metal. Note the different energy scales in both panels.

spots that we observed do not allow us to exclude the possibility that the hexagons expand slightly, distort, or rotate during growth. We may in fact expect this to happen as the nearest neighbor distance of the adsorbate at 1 ML is usually smaller than in the bulk of the alkali metals. The alkali metals must have a tendency to form their natural bcc structure, at least for very thick films.

IV. FILM VIBRATIONS

A. Dispersion curves of phonons in the film surface

We have prepared annealed films of various thicknesses and investigated the surface phonon modes by energy resolved helium scattering. The results for K/Ni(001) and Cs/Cu(111), shown in Fig. 5, display a number of similarities to the data for Na/Cu(001) which was published earlier.[8] The mode with the lowest energy has by far the largest excitation cross section and develops eventually into the surface Rayleigh mode as the film thickness increases. All other modes are weaker and show only little dispersion.

Dispersion and excitation cross sections for these modes in alkali-metal films have recently been investigated by employing slab calculations to model the lattice dynamics. In these calculations the film is assumed to be attached to a rigid substrate.[26] In the following we will concentrate on the long wavelength limit for the surface modes, where the atoms of a particular layer vibrate in phase. The large excitation cross sections indicate that these modes are polarized perpendicular to the substrate. This assumption is supported by the results of the slab calculation.

B. Film resonances

For both systems, K/Ni(001) and Cs/Cu(111), significant phonon excitation probabilities were observed which remained large in the limit of zero momentum transfer parallel to the film surface. This behavior is evidence for large vibrational amplitudes of the surface atoms perpendicular to the surface. In accordance with the explanation of a similar behavior in Na/Cu in Ref. 8, we interpret these modes as standing longitudinal bulk waves resulting from the large reflection coefficients [0.82, 0.91, and 0.89 for Na/Cu(001), K/Ni(001), and Cs/Cu(111), respectively] attributable to the acoustic impedance mismatch at each of the respective interfaces.[27] In Ref. 8 the standing waves were treated as having a node at the interface and an antinode at the surface, the surface atoms thus vibrating with large amplitude. In this picture, therefore, a quarter of the fundamental film mode wavelength matches the thickness of the film. The wave vectors perpendicular to the substrate, q_z, of the fundamental mode $(n=1)$ and the higher harmonics $(n>1)$ are

$$q_z(n,N)=\frac{2n-1}{N}\,\frac{\pi}{2d}, \tag{2}$$

where N stands for the number of layers, and d for the interlayer spacing.[8] The factor $(2n-1)/N$ was used to label the modes in Fig. 5. Obviously in this equation the interlayer spacing is assumed to be constant and equal to the distance of (110) planes in the bulk alkali metals.

From our experimental results we identify the lowest vibrational energy, measured for an N-layer film and for vanishing parallel momentum transfer (cf. the bottom panels of Fig. 5), with $\omega_1(N)$, the frequency of the fundamental film mode with the wave vector $q_z(n=1,N)$. The sequence of measured overtones $\omega_n(N)$, $(n>1)$ is then related to $q_z(n,N)$, the wave vectors of the higher harmonics. In this way one can obtain the dispersion of the longitudinal modes in the film propagating perpendicularly to the surface by plotting $\omega_n(N)$ against the wave vectors $q_z(n,N)$ calculated from Eq. (2). In Fig. 6 these curves are shown, the different symbols referring to different N, and are compared with the longitudinal alkali-metal bulk mode along the $\langle 110\rangle$ direction[28] depicted by the solid line. All points are seen to

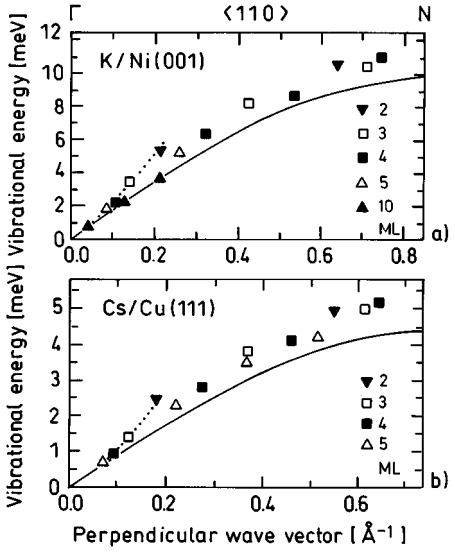

FIG. 6. Comparison of longitudinal bulk phonon dispersion curves along a direction perpendicular to the substrate surface (solid line from Ref. 28) with the properties of film modes (symbols of various shape). Vibrational energy of the longitudinal wave confined perpendicularly to the interface is identified with the measured film mode energy obtained for vanishing parallel momentum transfer; the wave vector of the confined mode is calculated from the wavelength according to Eq. (2). The dotted line connects the data for the fundamental film modes ($n=1$; see the text). Upper panel, K/Ni(001); lower panel, Cs/Cu(111).

lie above the dispersion curve for the bulk mode, as was found previously to be the case for the results from the Na/Cu(001) system, when plotted in the same manner.[8] However, for the Na/Cu(001) system all points, independent of their layer index N, were found to lie on a common curve, while the results of the present measurements (Fig. 6) show that for K/Ni(001) and Cs/Cu(111) the points corresponding to a particular film thickness N move closer to the bulk mode as N increases.

This observation cannot be explained within the framework of the simple model employed in Ref. 8, which assumes, among other things, an interfilm layer spacing independent of the number of layers deposited and which remains constant from layer to layer (no decrease of strain in the system during growth) and assumes that the node of the standing wave is located precisely at the interface (assumes that the film is attached to a completely rigid substrate). Both of these assumptions may be poorly satisfied for films of the heavier alkali metals.

For Na/Cu(001) the vibrational frequencies $\omega_n(N)$ of the fundamental mode and the overtones were found earlier[8] to be proportional to $1/N$, the inverse of the film thickness. This relationship in connection with Eq. (2) implies that $\omega_n(N)$ is directly proportional to the perpendicular wave vector $q_z(n,N)$ and implies thus a linear dispersion curve of the confined longitudinal bulk mode. The analogy between film modes and vibrational resonances in an open standing wave is justified in that the latter are also determined by Eq. (2) (in which Nd is replaced by the length of the organ pipe) and by a sound wave with linear dispersion.

In Figs. 6(a) and 6(b) the points referring to the fundamental modes ($n=1$) for different film thicknesses N are

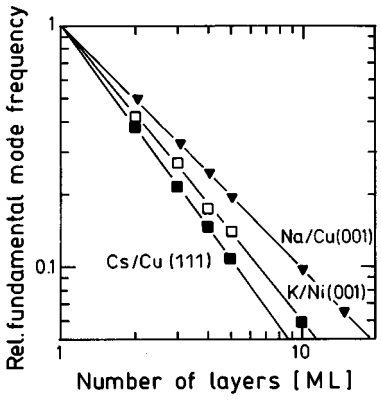

FIG. 7. Measured fundamental frequencies of film modes, normalized to 1 for 1 ML, for different film thicknesses. Various symbols refer to different systems. The log-log plot allows the determination of the exponent p, described in the text; $p=1$, as found for Na/Cu(001), refers to ''genuine'' open standing wave modes; this parameter is >1 in the cases of K/Ni(001) and Cs/Cu(111).

connected by a broken line. While for Na/Cu(001) this line was found to be straight in accordance with the linear dispersion of the confined bulk mode discussed above, for the heavier alkali metals the broken lines in Figs. 6(a) and 6(b) are curved. This curvature again indicates that the heavier adsorbate systems seem to be less well described by ''pure'' open standing wave behavior.

V. FILM STRAIN

The scaling of the organ pipe mode frequencies, $\omega_1(N)$, like $1/N$ for Na/Cu(001), is expected if the interface force constant happens to be exactly twice the value of the interlayer force constant in the alkali-metal film within the framework of the simple rigid substrate model derived in Ref. 11. In this model, if the interface force constant happens to be much smaller than the force constant in the film, the energy of the fundamental mode will depend on the number of layers like $1/\sqrt{N}$. In accordance with Ref. 11 we therefore generally assume a power law for the dependence of the fundamental frequencies on the number N of layers:

$$\omega_1(N)=\omega_1(1)N^{-p}. \tag{3}$$

The nature of the observed phonons for a 1 ML film is quite different from that of the thicker films and will be discussed elsewhere.[29] Thus data for the frequency $\omega_1(1)$ cannot be obtained from the experiments. It is related to the interface force constant, which is expected to change when the second layer is deposited. For a determination of the exponent p the value of $\omega_1(1)$ is not needed and in the plot of Fig. 7 we chose it such that all lines fall together in the top left corner. We obtain $p=1.01\pm0.01$, 1.23 ± 0.07, and 1.39 ± 0.01 for Na/Cu(001), K/Ni(001), and Cs/Cu(111), respectively.

Following the argument from above, the interface force constant for K/Ni(001) and Cs/Cu(111) seems to be larger than twice the interlayer force constant in the respective film. As a test, we determine p theoretically in the simple model of a linear chain of atoms attached at one end to a rigid substrate, with only nearest neighbor force constants (see also Ref. 30). The force constants in the chain have all the

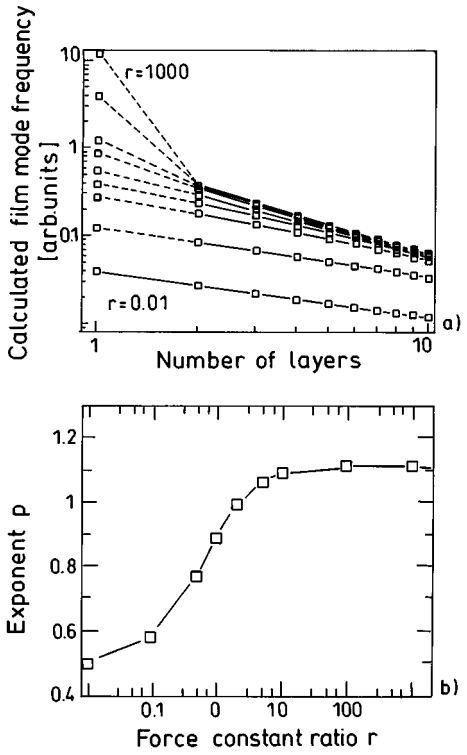

FIG. 8. Top panel: calculated ''fundamental frequencies of film modes'' for a film modeled by a linear chain attached at one end to a rigid substrate; see the text. The parameter distinguishing the different lines is the ratio r of the interface force constant α_i and the force constant in the ''film'' α_f. Note the linear behavior for $N>1$ ML in the log-log plot which confirms the algebraic formula discussed in the text. Bottom panel: the weak dependence of the exponent p in Eq. (3) on the ratio of force constants r; see the text.

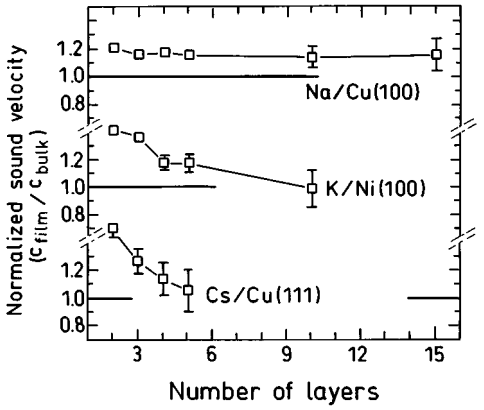

FIG. 9. Sound velocities during growth. Plotted is the ratio of the phase velocity of longitudinal waves, c_{film}, in the large wavelength limit propagating perpendicularly to the film and the corresponding sound velocity in the alkali-metal bulk, c_{bulk}, versus the film thickness.The points are obtained from the frequencies and wave vectors of the respective fundamental film mode. Obviously bulk properties in films of increasing thickness are more readily achieved for Cs/Cu than for K/Ni while the stress in the Na/Cu system prevails even in a thick film.

same value but may differ from the value of the force constant between chain and substrate. The calculated vibrational energies of the fundamental mode are plotted versus the number of layers in a semilogarithmic plot in Fig. 8(a). If one neglects the values for 1 ML the results seem to obey the postulated power law and values for p can be extracted for various ratios r of the interface force constant α_i to the interlayer force constant in the ''film,'' α_f. The results are plotted in Fig. 8(b) and demonstrate that p is extremely insensitive to this ratio if it exceeds 10. Moreover, the observed p values for K/Ni(001) and Cs/Cu(111) are far too large to be reasonably well explained by the simple model.

A possible explanation for the quantitatively large values of exponent p determined from the experiment, when compared with the predictions of the model above, is a decrease in strain occurring within the alkali-metal film as a function of the number of layers deposited during growth. Such an effect was not incorporated into the simple model employed above. Very strong evidence for the presence of such a strain relief during growth was provided by the results of our helium atom reflectivity measurements, described earlier in Sec. III B and presented graphically in Fig. 2, in which a strong layer dependence in the surface Debye temperature was observed for both the K/Ni(001) and Cs/Cu(111) systems.

We obtain the sound velocity in the long wavelength limit for the longitudinal standing wave perpendicular to the interface by dividing the measured film mode energy, $\omega_1(N)$, by the corresponding wave vector $q_z(1,N)$, which was estimated assuming a constant interlayer spacing. In Fig. 9 we compare the resulting sound velocities in the film with the sound velocities for the bulk longitudinal modes along the $\langle 110\rangle$ direction as determined by neutron scattering[28] (Na: 3740 m/s, K: 2735 m/s, Cs: 1380 m/s). The error bars are calculated assuming a constant uncertainty in the measured vibrational energies of about 0.1 meV.

In the sodium films the sound velocity is on average 20% higher than in the bulk and observed to be very weakly dependent of the film thickness. Thus the strain in the film is not significantly reduced during growth. In contrast, a considerable reduction in sound velocity with coverage for the potassium and cesium films is found (29% reduction in sound velocity for potassium and 33% for cesium) and the bulk values are reached after adding 10 layers in the case of K and only 5 layers for the Cs system. This effect cannot be accounted for in the simple models employed in this work. In the light of our Debye temperature measurements, we thus largely attribute the observed behavior to the presence of strain relief in the growth process. Our work suggests that the softer the alkali metal, the more pronounced its ability to bear and subsequently reduce strain.

The origin of the strain is the compressed hexagonal arrangement of the alkali-metal atoms at 1 ML with next neighbor separations a few percent less than in the bulk alkali metals. At least potassium and cesium seem to be soft enough to reduce this strain from layer to layer by laterally expanding to their natural separation.

VI. CONCLUSIONS

We have presented experimental data for the growth of potassium on Ni(001) and cesium on Cu(111). As for Na/

Cu(001) vibrational resonances in the alkali-metal films have been observed. The initially compressed films seem to relax during growth leading to interlayer force constants that depend on the film thickness.

Comparison of the data with our simple dynamical calculations shows that much more detailed calculations are required, in which the layer by layer reduction in strain is adequately modeled, in order to describe the data. Our results have thus demonstrated that HAS, when applied to the study of thin film growth, has the power to elucidate details of the interatomic forces not only at the surface but also between the inner adsorbate layers under investigation. This may be of particular relevance for the understanding of magnetic multilayers.

ACKNOWLEDGMENTS

We would like to thank Professor J.P. Toennies for stimulating discussions and for his hospitality to two of us (J.L. and A.R.). One of us (J.L) would like to kindly thank the Alexander von Humboldt Foundation for its financial support enabling his participation in the project. We also acknowledge many helpful discussions with our colleagues H.J. Schief, N.S. Luo, P. Ruggerone, and D. Fuhrmann.

*Present address: Atomic and Molecular Physics Laboratories, Research School of Physical Sciences and Engineering, ANU, Canberra ACT 0200, Australia.

[1] R.D. Diehl and R. McGrath, Surf. Rev. Lett. **2**, 387 (1995).

[2] A.B. Andrews, D.M. Riffe, and G.K. Wertheim, Phys. Rev. B **49**, 8396 (1994).

[3] G. Pacchioni and P.S. Bagus, Surf. Sci. **286**, 317 (1993).

[4] *Physics and Chemistry of Alkali Metal Adsorption*, Materials Science Monographs Vol. 57, edited by H.P. Bonzel, A.M. Bradshaw, and G. Ertl (Elsevier, Amsterdam, 1989).

[5] S. Andersson, J.B. Pendry, and P.M. Enchenique, Surf. Sci. **65**, 539 (1977).

[6] B.S. Itchkawitz, A.P. Baddorf, H.L. Davis, and E.W. Plummer, Phys. Rev. Lett. **68**, 2488 (1992).

[7] G.K. Wertheim, D.M. Riffe, and P.H. Citrin, Phys. Rev. B **49**, 2277 (1994).

[8] G. Benedek, J. Ellis, A. Reichmuth, P. Ruggerone, H. Schief, and J.P. Toennies, Phys. Rev. Lett. **69**, 2951 (1992).

[9] J. Cui, J.D. White, and R.D. Diehl, Surf. Sci. **293**, L841 (1993).

[10] J.D. White, J. Cui, M. Strauss, R.D. Diehl, F. Ancilotto, and F. Toigo, Surf. Sci. **307/309**, 1134 (1994).

[11] N.S. Luo, P. Ruggerone, J.P. Toennies, G. Benedek, and V. Celli, J. Electron Spectrosc. Relat. Phenom. **64/65**, 755 (1993).

[12] H.-J. Ernst, E. Hulpke, and J.P. Toennies, Phys. Rev. B **46**, 16 081 (1992).

[13] H.J. Schief, Diploma thesis, University of Göttingen (1990).

[14] J.J. de Miguel, A. Cebollada, J.M. Gallego, J. Ferrón, and S. Ferrer, J. Cryst. Growth **88**, 442 (1988).

[15] B.J. Hinch, C. Koziol, J.P. Toennies, and G. Zhang, Europhys. Lett. **10**, 341 (1989).

[16] G. Rosenfeld, R. Servaty, Ch. Teichert, B. Poelsema, and G. Comsa, Phys. Rev. Lett. **71**, 895 (1993).

[17] W.R. Tyson and W.A. Miller, Surf. Sci. **62**, 267 (1977).

[18] E. Bauer, Z. Kristallogr. **110**, 372 (1958).

[19] J.R. Manson, Phys. Rev. B **43**, 6924 (1991).

[20] N.W. Ashcroft and N.D. Mermin, *Solid State Physics* (W. B. Saunders, Philadelphia, 1976).

[21] For a sufficiently low defect concentration n the Debye-Waller corrected reflectivity R plotted in Fig. 3 can be written as a linear function in n:

$$R = 1 - \frac{n}{n_0}.$$

Assuming that the rate with which the defects are removed is proportional to their number, n, a temperature independent attempt frequency, ν, and the usual Boltzmann factor containing the energy barrier, E_b,

$$\frac{\partial n}{\partial t} = -n\nu e^{-E_b/kT},$$

and that the temperature T is varied linearly with time ($\partial T/\partial t =$ const) one can calculate $n' = \partial n/\partial T$ and $n'' = \partial^2 n/\partial T^2$. At $T_{1/2}$ the curve $R(T)$ exhibits a point of inflection ($n'' = 0$) and the slope of $R(T)$ at this point is determined by $T_{1/2}$ and ΔT. Thus the number of defects and its derivatives with respect to T are given by

$$n''(T_{1/2}) = 0,$$
$$n'(T_{1/2}) = n_0/\Delta T,$$
$$n(T_{1/2}) = n_0/2,$$

and one obtains the following estimate for the energy barrier:

$$E_b = 2\frac{T_{1/2}}{\Delta T} kT_{1/2} \quad \text{or} \quad E_b(\text{meV}) = 0.172\frac{T_{1/2}^2(\text{K})}{\Delta T(\text{K})}.$$

[22] J. Ellis and J.P. Toennies, Phys. Rev. Lett. **70**, 2118 (1993).

[23] Taruga, H. Tochihara, and Y. Murata, Phys. Rev. Lett. **52**, 1794 (1984).

[24] D. Fischer and R.D. Diehl, Phys. Rev. B **46**, 2512 (1992).

[25] D. Fuhrmann, Diploma thesis, University of Göttingen, 1995.

[26] N.S. Luo (unpublished).

[27] The acoustic impedance is defined as mass density times longitudinal sound velocity perpendicular to the interface. The reflection coefficient can be obtained by dividing the difference in impedances at the interface by their sum. The numbers are calculated from data in Ref. 29 and in the *American Institute of Physics Handbook*, 3rd. ed., edited by D.E. Gray (McGraw-Hill, New York, 1972).

[28] *Landolt-Börnstein, Numerical Data and Functional Relationships in Science and Technology*, edited by H. Hellwege (Springer, Berlin, 1981) Band 13, Teil a.

[29] E. Hulpke and A. Reichmuth (unpublished).

[30] N.S. Luo, P. Ruggerone, and J.P. Toennies (unpublished).